Instantaneous frequency computation: theory and practice

Matthew J. Yedlin[1], Gary F. Margrave[2], and Yochai Ben Horin[3]

ABSTRACT

We present a review of the classical concept of instantaneous frequency, obtained by differentiating the instantaneous phase and also show how the instantaneous frequency can be computed as the first frequency moment of the Gabor or Stockwell transform power spectrum. Sample calculations are presented for a chirp, two sine waves, a geostationary reflectivity trace and a very large quarry blast. The results obtained clearly demonstrate the failure of the classical instantaneous frequency computation via differentiation of the instantaneous phase, the necessity to use smoothing and the advantage of the first moment computation which always results in a positive instantaneous frequency as a function of time. This research points to the necessity of devising an objective means to obtain optimal smoothing parameters. Future work will focus on using linear and nonlinear inverse theory to achieve this goal.

INTRODUCTION

While the concept of frequency is very old, dating back to Pythagoras,(529-570 B.C.), creator of the Pythagorean scale, a system of tuning that was used until the early 1500's, the concept of instantaneous frequency is relatively new, originating with Nobel Laureate, Dennis Gabor (Gabor, 1946). In exploration seismology, instantaneous frequency has been used as one of number of seismic attributes, beginning with the work of Taner (Taner et al., 1979) and extended by Barnes (1992, 1993), In electrical engineering, an excellent review of the theory and application of the instantaneous frequency is provided by Boashash (1992a,b).

In this research work, we will first review the basic theory of the classical method of computing the instantaneous frequency in the continuous domain. Then we will review an application of a technique developed by Fomel (Fomel, 2007b) to address the smoothing issues arising in the computation of the instantaneous frequency. We will then present the method using the moments of the linear time-frequency transforms as applied by Margrave (Margrave et al., 2005) and Stockwell (Stockwell et al., 1996). In addition to the linear time-frequency transform analysis, there exists the bi-linear Wigner-Ville transform Wigner (1932); Ville et al. (1948), which has also been applied to dispersive signal detection in earthquake records (Prieto et al., 2005). This bi-linear transform will not be considered in the present research scope.

[1]Department of Electrical and Computer Engineering, University of British Columbia
[2]Geoscience, University of Calgary
[3]SOREQ, Yavneh, Israel

THEORY

Classical Instantaneous Phase

The classical instantaneous phase originates with phase modulation concepts (Boashash, 1992a,b), in which the signal, $f(t)$, has a representation of the form,

$$f(t) = amplitude(t)e^{i\omega_0 t + i\int_0^t mod(\tau)\,d\tau}. \tag{1}$$

In (1), $amplitude(t)$, is a very slowly-varying function of time, with ω_0 the carrier frequency, with $mod(\tau)$ a slowly-varying modulation function. Thus the signal $f(t)$ does not look very different from the basic exponential,

$$e^{i\,\omega_0\,t} = \cos(\,\omega_0\,t) + \sin(\,\omega_0\,t), \tag{2}$$

which is represented graphically in polar form as a rotating vector with instantaneous angular frequency, ω_0.

The above can be generalized to a general complex signal, known as the analytic signal, given by

$$A(t) = f(t) + i\mathcal{H}[f(t)] = f(t) + ig(t) \tag{3}$$

where $g(t)$ is obtained by the Hilbert transform (see **APPENDIX**), a convolution operation defined by

$$g(t) = \int_{-\infty}^{\infty} f(\tau)\,\frac{1}{\pi(t-\tau)}\,d\tau. \tag{4}$$

Basically the Hilbert transform maps cosines into sines and sines into negative cosines. Thus each Fourier transform component is phase rotated by $\frac{\pi}{2}$, with positive frequency components phase-delayed by $\frac{\pi}{2}$ and negative frequency components phase-advanced by $\frac{\pi}{2}$. The resultant inverse Fourier transform of this phase rotation yields the Hilbert transform. The application of the Hilbert transform to whole earth seismology, as an arrival diagnostic is elegantly presented in the paper by Choy and Richards (Choy and Richards, 1975), titled "Pulse distortion and Hilbert transformation in multiply reflected and refracted body waves".

From (3), $A(t)$ can be written in polar form with magnitude $Env(t)$ and phase, $\Phi(t)$ given by

$$\begin{aligned} A(t) &= f(t) + ig(t) = Env(t)\ \exp\left[i\Phi(t)\right], \quad \text{where} && (5)\\ Env(t) &= \sqrt{f(t)^2 + g(t)^2}, \quad \text{and} && (6)\\ \Phi(t) &= \tan^{-1}\left[\frac{g(t)}{f(t)}\right] && (7) \end{aligned}$$

From the foregoing, following the electrical engineering literature in communication theory Wikipedia (2013), we can write that

$$\begin{aligned} f(t) &= I(t) = Env(t)\ \cos[\Phi(t)], \quad \text{and} && (8)\\ g(t) &= Q(t) = Env(t)\ \sin[\Phi(t)] \quad \text{where} && (9) \end{aligned}$$

$I(t)$ is denoted as the in-phase component of the analytic signal and $Q(t)$ is denoted as the quadrature component.

We can differentiate (7) with respect to time by simple application of the chain rule to obtain the instantaneous angular frequency (IAF), $\Omega(t)$, given by

$$\Omega(t) = \frac{d\,\Phi(t)}{dt} = \frac{n(t)}{d(t)} = \frac{f(t)\dfrac{d}{dt}g(t) - g(t)\dfrac{d}{dt}f(t)}{f(t)^2 + g(t)^2}. \tag{10}$$

This estimate is divided by 2π to obtain the instantaneous frequency.

We can anticipate the following problems in the computation of the instantaneous frequency (IF) from (10). First, the denominator, $d(t)$, the envelope squared, may approach zero at various times. Second, the numerator $n(t)$ is composed of a difference of the pair-wise multiplication of two signals, involving both the differentiation operation and convolution with the Hilbert kernel, $\dfrac{1}{\pi t}$. All of the above amplify the noise. Furthermore, point-wise computation of the instantaneous frequency is somewhat paradoxical, given that in general, we need an time-interval to estimate frequency. A partial solution to these problems is outlined in the following section.

Smoothed Classical Instantaneous Phase – Local Frequency

Fomel (2007a,b) has initiated a technique to address the noise amplification issues. The origin of this analysis stems from previous work with Claerbout (Fomel and Claerbout, 2003) and was also employed by Liu (Liu et al., 2011).

To facilitate the development of Fomel's technique we redefine our signals in discrete time and cast our instantaneous frequency, $\Omega(t)$, as computed in (10), in matrix-vector form. In what follows, the variable, t will be implicitly associated with the vector indices. Using Fomel's notation, $n(t)$ in (10) will be written as $\mathbf{n}$. In addition, we define $\mathbf{f}$ as the discrete version of $\Omega(t)$ divided by 2π and represent the point-wise division of the two signals in (10) as a matrix-vector operation given by

$$\mathbf{f} = \mathbf{D^{-1}n}, \tag{11}$$

where $\mathbf{D}$ is a diagonal matrix whose elements are the discrete time values of the envelope squared multiplied by 2π. As Fomel points out, due to the envelope squared possibly approaching zero, the inverse must be regularized. A straightforward way to do that is use a Marquardt type of regularization. Thus we modify (11) and propose to calculate $\mathbf{f}$ by writing that

$$\mathbf{f} = \left(\mathbf{D} + \epsilon^{\mathbf{2}}\mathbf{R}\right)^{\mathbf{-1}}\mathbf{n}, \tag{12}$$

where $\mathbf{R}$ is the matrix representation of a regularizing operator. In his paper on shape regularization, (Fomel, 2007b), Fomel writes the regularization operator $\mathbf{R}$ in terms of a smoothing operator $\mathbf{S}$, as

$$\mathbf{S} = \left(\mathbf{I} + \epsilon^{\mathbf{2}}\mathbf{R}\right)^{\mathbf{-1}}, \tag{13}$$

and then after scaling by λ, writes the estimated instantaneous frequency (now smoothed) $\mathbf{f_{loc}}$ as

$$\mathbf{f_{loc}} = \left[\lambda^2\mathbf{I} + \mathbf{S}\left(\mathbf{D} - \lambda^2\mathbf{I}\right)\right]^{-1}\mathbf{S}\mathbf{n}, \tag{14}$$

It is (14) that we will use for calculating a local rather than instantaneous frequency in the section **PRACTICE**.

First Moment Computation of the Local Frequency

An alternative to the Fomel smoothing technique is provided in the book by Cohen (Cohen, 1995). He presents an estimate of the local frequency by taking the frequency moment of a time-frequency transform. Thus the local frequency, f_{loc}, which we will use in the section **PRACTICE**, is given in continuous time, by

$$f_{loc} = \frac{1}{\int |S(t,f)|^2\, df} \int f\, |S(t,f)|^2\, df. \tag{15}$$

In (15), the time-frequency transform, $S(t,f)$, can be computed using either the Gabor transform or the Stockwell transform. These are both given here for completeness:

$$\begin{aligned} S_{Gabor}(t,f) &= \int_{-\infty}^{\infty} g(\tau)\ |f|\ win(\tau - t) e^{-i\,2\pi f\tau} d\tau \text{ and} && (16)\\ S_{Stockwell}(t,f) &= \frac{1}{\sqrt{2\pi}} \int_{-\infty}^{\infty} g(\tau)\ |f|\ e^{[-(t-\tau)^2\, f^2]/2} e^{-i\,2\pi f\tau} d\tau, && (17) \end{aligned}$$

where $g(t)$ is our seismic trace, and in (16), $win(t)$ is chosen to be a fixed-width Gaussian window. We note that the Stockwell transform's window is also Gaussian, whose width decreases as the frequency increases. For both moment computations, the integrals are performed over the signal bandwidth.

PRACTICE

We now apply the theory to four different signals:

1. A linear chirp.
2. Two sine waves.
3. A non-stationary trace.
4. A quarry blast.

The results are presented in the following four figures which clearly demonstrate the usefulness of the instantaneous frequency. For the computations, we use (10) for the instantaneous frequency, (14) for Fomel's f_{loc} and (15) for f_{loc} obtained using the time-frequency moments, obtained from either the Gabor or Stockwell transforms. All frequency axes have units of Hz.

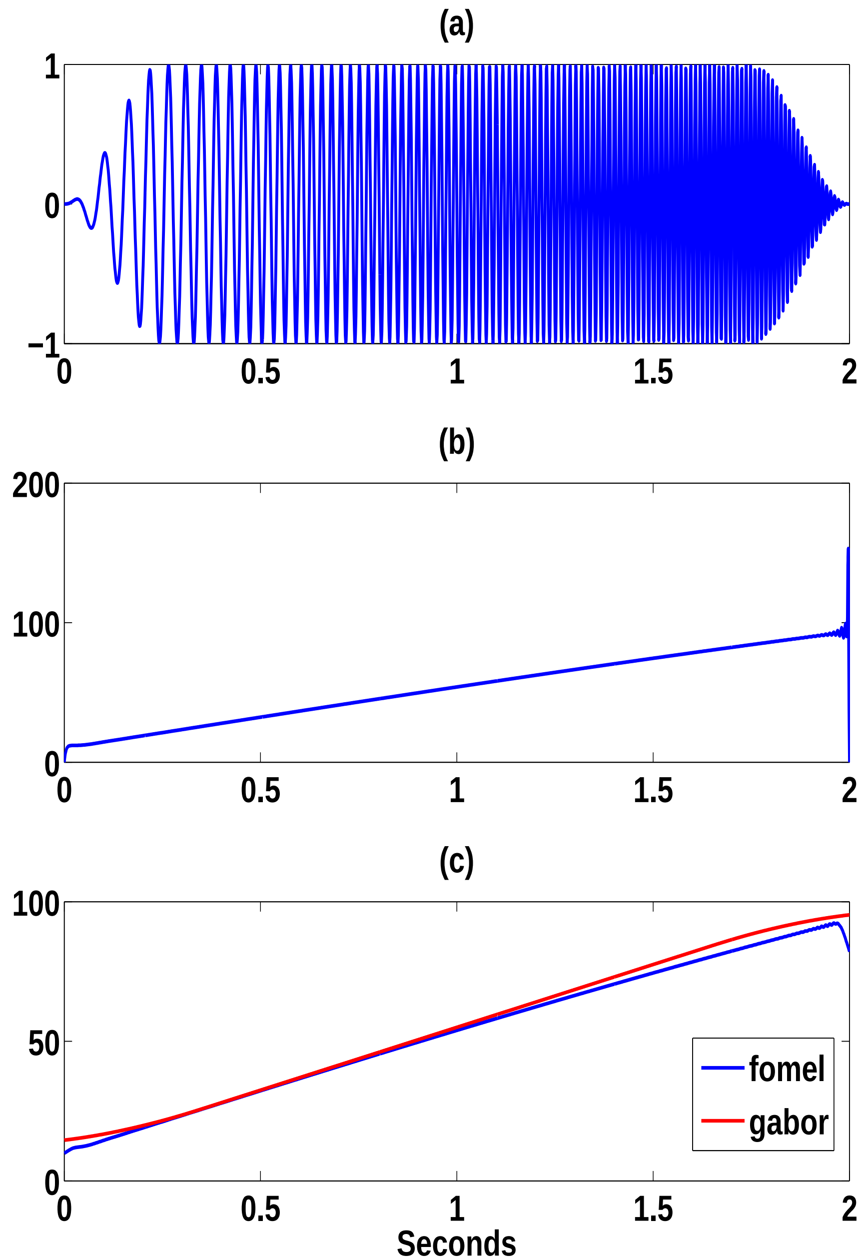

FIG 1.

Panel (a) : Linear Chirp – 10 to 100 Hz
Panel (b) : Instantaneous Frequency
Panel (c) : Fomel's f_{loc} and Gabor's f_{loc}.

text
text

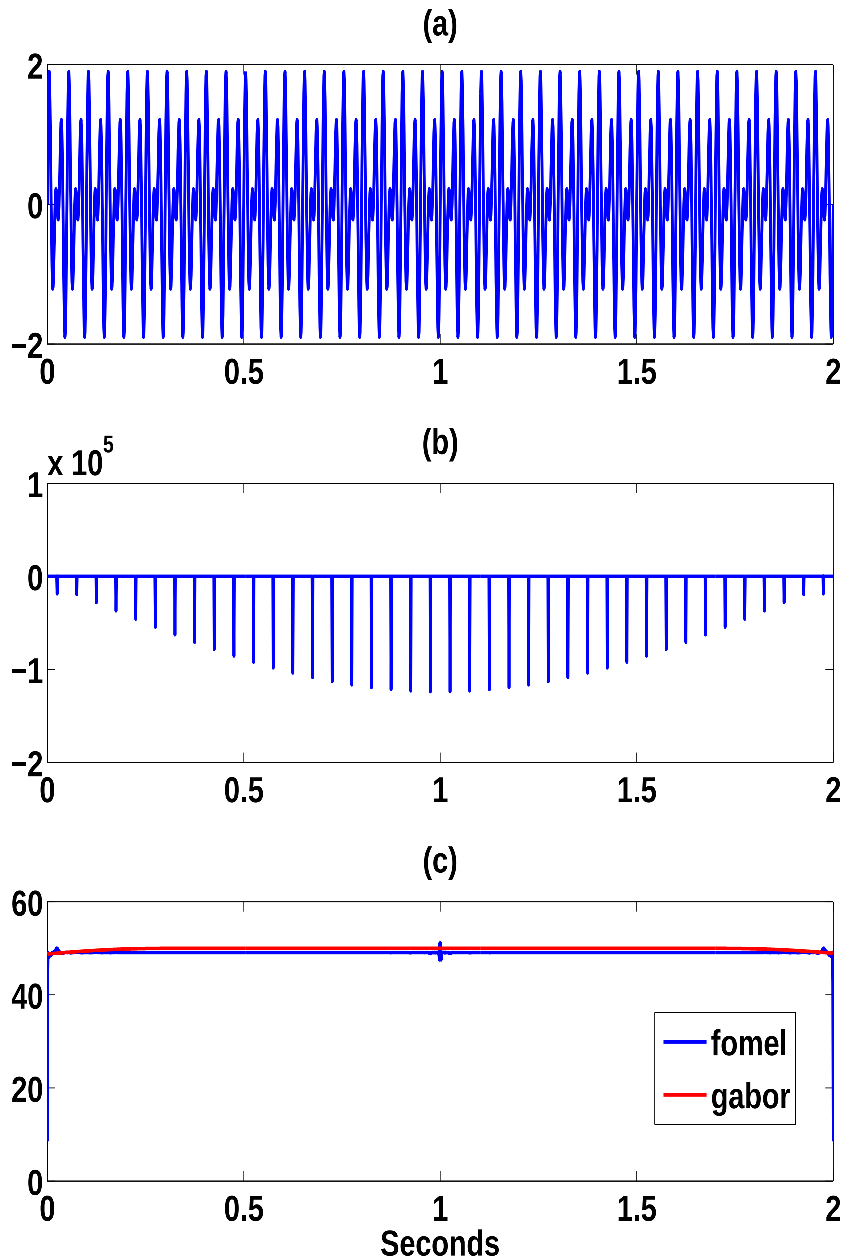

FIG 2.

Panel (a) : Two sine waves: 40 and 60 Hz
Panel (b) : Instantaneous Frequency
Panel (c) : Fomel's f_{loc} and Gabor's f_{loc}.

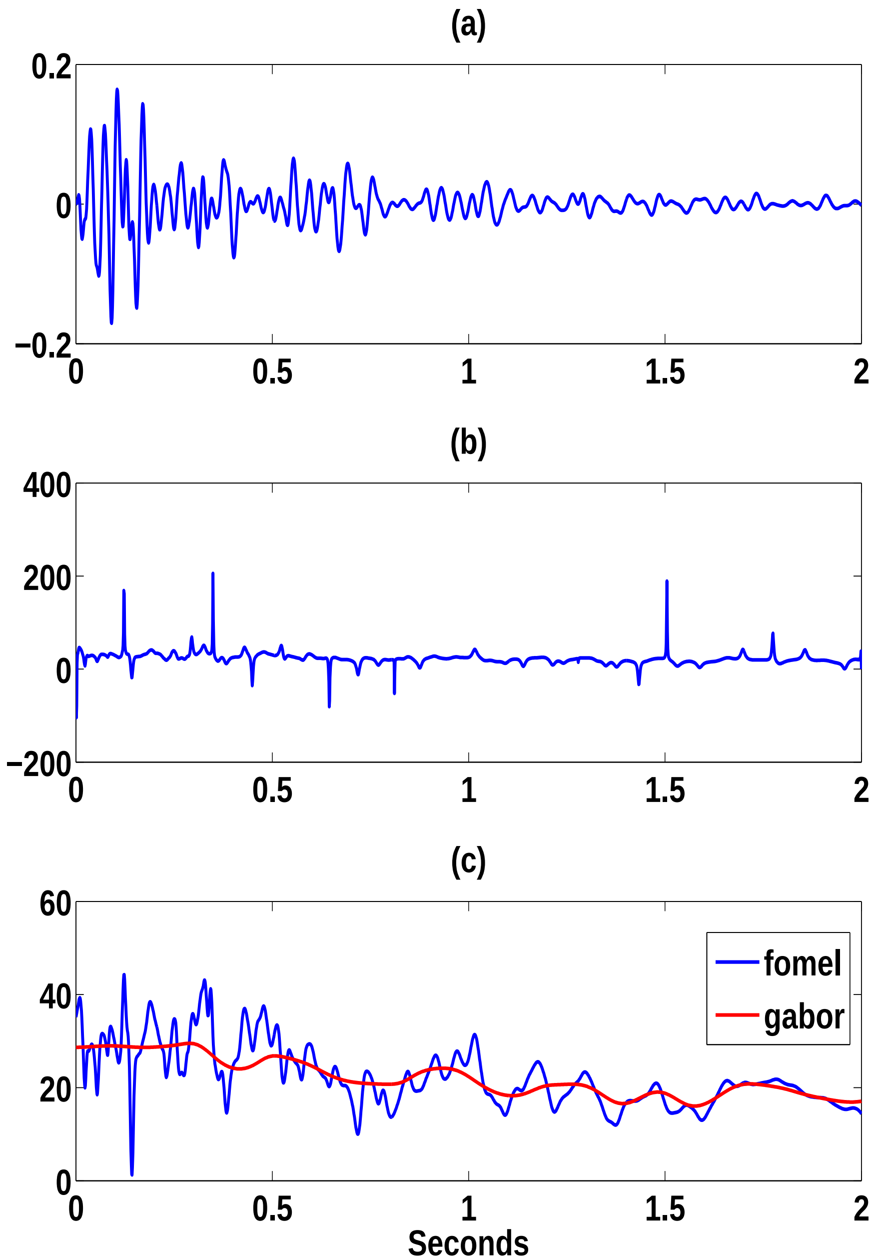

FIG 3.

Panel (a) : Nonstationary Seismic Signal
Panel (b) : Instantaneous Frequency
Panel (c) : Fomel's f_{loc} and Gabor's f_{loc}.

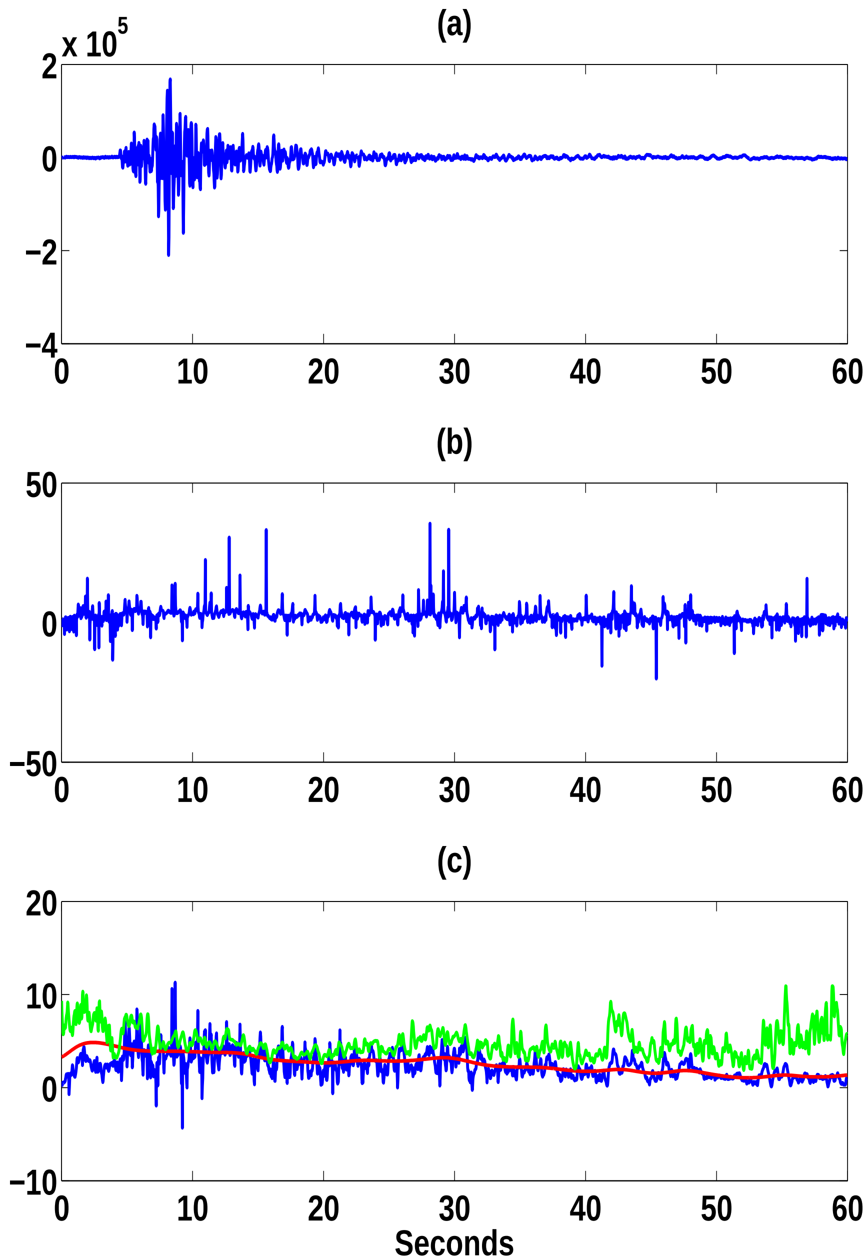

FIG 4.

Panel (a) : 10^4kg TNT Quarry Blast

Panel (b) : Instantaneous Frequency

Panel (c) : Fomel's f_{loc}, Gabor's f_{loc} and Stockwell's f_{loc}.

In Fig. 1, we have generated a linear chirp signal with frequency range 10 to 100 Hz. We clearly see that the instantaneous frequency and f_{loc} computed via either Fomel's method or the frequency-moment method yield the same results. In the frequency-moment method, there is a slight discrepancy due to edge effects. This edge-effect is clear on all the examples.

In Fig. 2, composed of the sum of two sine waves of 40 and 60 Hz, there is clear departure between the instantaneous frequency calculation in Panel(b) and f_{loc} of Panel(c). The correct instantaneous frequency is 50 Hz, which is correctly demonstrated in Panel(c). Panel(b), the classical instantaneous frequency, is completely dominated by artifacts due to the numerical instability of dividing by the envelope squared in (10). In fact, between the erroneous impulses in Panel(b), the value of the instantaneous frequency is 50 Hz, which is not apparent due to the scale distortion. Furthermore, the instantaneous frequency artifacts are negative, a non-physical result.

Panel(a) of Fig. 3 is a non-stationary seismic trace, our first realistic simulation example. Again the classical instantaneous frequency shown in Panel(b) has artifact impulses and negative values. The curves of f_{loc} in Panel(c) are comparable, with f_{loc} obtained via the Gabor transform, much smoother, due to the wide size of the Gaussian window chosen. The Fomel method results in a somewhat noisier result that depends on the size of the smoothing window and scale factor, λ. We have found that it is not easy to choose these values to obtain results that are close to f_{loc} obtained using the frequency-moment calculation. The general trend in frequency as a function of time, shown in Panel(c) was verified by computing a windowed frequency spectrum for a number of different window positions along the trace.

In Fig. 4 we present the analysis from a quarry blast near Malkishua, Israel, consisting of 20000 kg of AFNO (ammonium nitrate) explosive, which has an approximate TNT equivalent of 10000 kg. Panel(a) shows the data from the blast, which has a highly non-stationary character. The signal begins with high frequency noise, then the main explosion arrival with high frequency surface waves, whose frequency content decays with time until the noise reappears. The instantaneous frequency shown in Panel(b) is again artifact-dominated. In Panel(c), we compare three measures of f_{loc}: Fomel's method, the Gabor frequency-moment computation and the Stockwell frequency-moment computation. All three behave in a similar fashion. The Gabor curve is the smoothest and generally agrees with the Fomel curve. The Fomel curve does go negative near 10 seconds. The Stockwell curve is shifted up from the other two curves, has a similar character to the Fomel curve, and clearly shows the return of the high frequency noise just after 40 seconds. This data set is clearly a challenge for the estimation of the instantaneous frequency as a function of time, regardless of the methods chosen.

CONCLUSIONS

We have presented three techniques to compute the instantaneous frequency attribute:

1. The classical method based on the direct differentiation of the instantaneous phase;
2. A smoothed version of the classical method based on a regularization technique devised by Fomel (Fomel, 2007b);
3. A frequency-moment method based on integration of the time-frequency spectrum

obtained using either the Gabor or Stockwell transform.

From the examples, it is clear that the classical method fails except in very simple situations, a fact also alluded to by Fomel (Fomel, 2007a). The most stable computations, that never go negative, are the frequency-moment computations, based on either the Gabor or Stockwell transforms. Future work will focus on an objective means of choosing the smoothing parameters in both the Fomel and frequency-moment methods, in order to obtain consistent results.

APPENDIX-HILBERT TRANSFORM

The Hilbert transform of a function, $\mathcal{H}[f(t)]$ is given by

$$\mathcal{H}[f(t)] = \int_{-\infty}^{\infty} f(\tau)\, \frac{1}{\pi(t-\tau)}\, d\tau. \tag{A-1}$$

We see that the Hilbert transform is the convolution of the function $f(t)$ with the Hilbert kernel, $1/\pi\, t$. In the frequency domain, the Hilbert transform is the product of the Fourier transform of $f(t)$ and the Fourier transform of $1/\pi\, t$. In this analysis of the Hilbert transform, it is much easier to get an intuitive understanding in the frequency domain, so we shall focus on explicitly obtaining the Fourier transform of the Hilbert kernel, $1/\pi\, t$, which we will denote by $k(t)$

The Fourier transform of $\mathcal{F}[k(t)]$ is given by

$$\mathcal{F}[k(t)] = \int_{-\infty}^{\infty} \frac{1}{\pi\, t} e^{-i\omega t}\, dt \tag{A-2}$$

$$= \underbrace{\int_{-\infty}^{\infty} \frac{\cos(\omega\, t)}{\pi\, t} dt}_{I_1} - \; i \underbrace{\int_{-\infty}^{\infty} \frac{\sin(\omega\, t)}{\pi\, t} dt}_{I_2} \tag{A-3}$$

Now let's look at the integrals I_1 and I_2.

The integrand in I_1 is odd over a symmetric interval and thus its value is zero. However, there is a mathematical formality in obtaining this result, since the integrand goes to infinity at $t = 0$. However, due to the anti-symmetry of $1/t$, and by using an appropriate limiting process, the positive and negative infinities cancel. This is what formal mathematics calls the P.V. or Principal Value of an integral.

We now turn to I_2, whose integrand is even and well-behaved at zero, where it approaches 1. Thus we have,

$$I_2 = -i \int_{-\infty}^{\infty} \frac{\sin(\omega\, t)}{\pi\, t} dt \tag{A-4}$$

$$= \frac{-2i}{\pi} \int_{0}^{\infty} \frac{\sin(\omega\, t)}{t}\, dt = \frac{-2i}{\pi}\, I_3 \tag{A-5}$$

It is not clear how to evaluate I_3 at this point. Normally one uses the method of residues of complex variables. We will assume only first year calculus and use a clever limiting process. The technique presented below was shown to Yedlin in 1968 by R.G. Sinclair, an excellent first year calculus professor at the University of Alberta.

To do the evaluation of I_3, we first create a new integral, $I_4(\alpha)$, given by

$$I_4(\alpha) = \int_{0}^{\infty} \frac{\sin(\omega\, t)}{t} e^{-\alpha\, t}\, dt, \tag{A-6}$$

where α is a parameter. Then we have that

$$\lim_{\alpha\to 0} I_4(\alpha) = I_3 \text{ and} \tag{A-7}$$

$$\lim_{\alpha\to \infty} I_4(\alpha) = 0 \tag{A-8}$$

Since $I_4(\alpha)$ is smooth, convergent function of α, we can differentiate it with respect to α to obtain

$$\frac{d\, I_4(\alpha)}{d\, \alpha} = \frac{d}{d\, \alpha} \int_{0}^{\infty} \frac{\sin(\omega\, t)}{t} e^{-\alpha\, t}\, dt \tag{A-9}$$

$$= \int_{0}^{\infty} \frac{\sin(\omega\, t)}{t} \frac{d}{d\, \alpha} \left[e^{-\alpha\, t} \right]\, dt \tag{A-10}$$

$$= -\int_{0}^{\infty} \sin(\omega\, t) e^{-\alpha\, t}\, dt, \tag{A-11}$$

which we can easily integrate by using integration by parts twice, or consulting a table of Laplace transforms. Thus we obtain

$$\frac{d\, I_4(\alpha)}{d\, \alpha} = -\frac{\omega}{\alpha^2 + \omega^2}, \tag{A-12}$$

which, by simple integration over α, results in

$$I_4(\alpha) = -\tan^{-1}\left(\frac{\alpha}{\omega}\right) + constant. \tag{A-13}$$

Now use the limit given by (A-8). For $\omega > 0$, $\tan^{-1}(\infty) = \pi/2$ and the constant is $\pi/2$ and when $\omega < 0$, the constant is -$\pi/2$. Finally, we have that

$$I_4(\alpha) = -\tan^{-1}\left(\frac{\alpha}{\omega}\right) + sgn(\omega)\frac{\pi}{2}. \tag{A-14}$$

We now apply the limit given (A-7) to get the final value for I_3 as

$$I_3 = sgn(\omega)\frac{\pi}{2}. \tag{A-15}$$

Finally we obtain the value for I_2, which is the Fourier transform of $1/(\pi t)$ and given by

$$I_2 = \frac{-2i}{\pi} I_3 = \frac{-2i}{\pi} sgn(\omega)\frac{\pi}{2} = -isgn(\omega) \tag{A-16}$$

which is our required Fourier transform for the Hilbert kernel $k(t)$.

One standard time series result emerges from the foregoing analysis. In the frequency domain, the analytic signal, $A(\omega)$ associated with a function $f(t)$ having Fourier transform $F(\omega)$ is given by

$$A(\omega) = [1 + i(-isgn(\omega)]F(\omega) = [1 + sgn(\omega)]F(\omega) \tag{A-17}$$

From the above result, we see that a quick way to obtain the analytic signal is first to take the Fourier transform of the time signal, then double all positive Fourier transform values, zero out the negative values, and then perform an inverse Fourier transform. The real part of the resulting inverse is the original signal and the imaginary part is its Hilbert transform.

REFERENCES

Barnes, A. E., 1992, The calculation of instantaneous frequency and instantaneous bandwidth: Geophysics, **57**, No. 11, 1520–1524.

Barnes, A. E., 1993, Instantaneous spectral bandwidth and dominant frequency with applications to seismic reflection data: Geophysics, **58**, No. 3, 419–428.

Boashash, B., 1992a, Estimating and interpreting the instantaneous frequency of a signal. i. fundamentals: Proceedings of the IEEE, **80**, No. 4, 520–538.

Boashash, B., 1992b, Estimating and interpreting the instantaneous frequency of a signal. ii. algorithms and applications: Proceedings of the IEEE, **80**, No. 4, 540–568.

Choy, G. L., and Richards, P. G., 1975, Pulse distortion and hilbert transformation in multiply reflected and refracted body waves: Bulletin of the Seismological Society of America, **65**, No. 1, 55–70.

Cohen, L., 1995, Time-frequency analysis, vol. 778: Prentice Hall PTR New Jersey.

Fomel, S., 2007a, Local seismic attributes: Geophysics, **72**, No. 3, A29–A33.

Fomel, S., 2007b, Shaping regularization in geophysical-estimation problems: Geophysics, **72**, No. 2, R29–R36.

Fomel, S., and Claerbout, J. F., 2003, Multidimensional recursive filter preconditioning in geophysical estimation problems: Geophysics, **68**, No. 2, 577–588.

Gabor, D., 1946, Theory of communication. part 1: The analysis of information, part 2: The analysis of hearing, part 3: Frequency compression and expansion: Electrical Engineers - Part III: Radio and Communication Engineering, Journal of the Institution of, **93**, No. 26, 429–457.

Liu, G., Fomel, S., and Chen, X., 2011, Time-frequency analysis of seismic data using local attributes: Geophysics, **76**, No. 6, P23–P34.

Margrave, G. F., Gibson, P. C., Grossman, J. P., Henley, D. C., Iliescu, V., and Lamoureux, M. P., 2005, The gabor transform, pseudodifferential operators, and seismic deconvolution: Integrated Computer-Aided Engineering, **12**, No. 1, 43–55.

Prieto, G. A., Vernon, F. L., Masters, G., and Thomson, D. J., 2005, Multitaper wigner-ville spectrum for detecting dispersive signals from earthquake records, *in* Conference Record of the Thirty-Ninth Asilomar Conference on Signals, Systems and Computers, 938–941.

Stockwell, R. G., Mansinha, L., and Lowe, R., 1996, Localization of the complex spectrum: the s transform: Signal Processing, IEEE Transactions on, **44**, No. 4, 998–1001.

Taner, M. T., Koehler, F., and Sheriff, R., 1979, Complex seismic trace analysis: Geophysics, **44**, No. 6, 1041–1063.

Ville, J. d. et al., 1948, Théorie et applications de la notion de signal analytique: Cables et transmission, **2**, No. 1, 61–74.

Wigner, E., 1932, On the quantum correction for thermodynamic equilibrium: Phys. Rev., **40**, No. 5, 749–759.

Wikipedia, 2013, In-phase and quadrature components, `http://en.wikipedia.org/wiki/In-phase_and_quadrature_components`, accessed: 2013-11-24.